

**Theory of periodic swarming of bacteria: Application to *Proteus mirabilis***A. Czirik,<sup>1,2,\*</sup> M. Matsushita,<sup>2,3</sup> and T. Vicsek<sup>1,2</sup><sup>1</sup>*Department of Biological Physics, Eötvös University, 1117 Budapest, Pázmány stny 1A, Hungary*<sup>2</sup>*Institute for Advanced Study, Collegium Budapest, 1014 Budapest, Szentháromság u 2, Hungary*<sup>3</sup>*Department of Physics, Chuo University, Kasuga, Bunkyo-ku, Tokyo 112-8551, Japan*

(Received 28 July 2000; published 27 February 2001)

The periodic swarming of bacteria is one of the simplest examples for pattern formation produced by the self-organized collective behavior of a large number of organisms. In the spectacular colonies of *Proteus mirabilis* (the most common species exhibiting this type of growth), a series of concentric rings are developed as the bacteria multiply and swarm following a scenario that periodically repeats itself. We have developed a theoretical description for this process in order to obtain a deeper insight into some of the typical processes governing the phenomena in systems of many interacting living units. Our approach is based on simple assumptions directly related to the latest experimental observations on colony formation under various conditions. The corresponding one-dimensional model consists of two coupled differential equations investigated here both by numerical integrations and by analyzing the various expressions obtained from these equations using a few natural assumptions about the parameters of the model. We determine the phase diagram corresponding to systems exhibiting periodic swarming, and discuss in detail how the various stages of the colony development can be interpreted in our framework. We point out that all of our theoretical results are in excellent agreement with the complete set of available observations. Thus the present study represents one of the few examples where self-organized biological pattern formation is understood within a relatively simple theoretical approach, leading to results and predictions fully compatible with experiments.

DOI: 10.1103/PhysRevE.63.031915

PACS number(s): 87.10.+e, 87.18.Hf

**I. INTRODUCTION**

To gain insight into the development and dynamics of various multicellular assemblies, we must understand how cellular interactions build up the structure and result in certain functions at the macroscopic, multicellular level. Microorganism colonies are one of the simplest systems consisting of many interacting cells and exhibiting a nontrivial macroscopic behavior. Therefore, a number of recent studies focused on experimental and theoretical aspects of colony formation and the related collective behavior of microorganisms [1,2].

The *swarming* cycles exhibited by many bacterial species, notably *Proteus (P.) mirabilis*, have been known for over a century [3]. When *Proteus* cells are inoculated on the surface of a suitable hard agar medium, they grow as short “vegetative” rods. After a certain time, however, cells start to differentiate at the colony margin into long “swarmer” cells possessing up to 50 times more flagella per unit cell surface area. These swarmer cells migrate rapidly away from the colony until they stop, and revert by a series of cell fissions into the vegetative cell form, in a process termed *consolidation*. The resulting vegetative cells grow normally for a time then swarmer cell differentiation is initiated in the outermost zone (terrace), and the process continues in periodic cycles resulting in a colony with concentric zonation depicted in Fig 1. A similar cyclic behavior was observed in an increasing number of Gram-negative and Gram-positive genera including *Proteus*, *Vibrio*, *Serratia*, *Bacillus*, and *Clostridium* (for reviews, see Refs. [4–6]).

The reproducibility and regularity of swarming cycles, together with the finding that its occurrence is not limited to a single species, suggest that periodic swarming phenomena can be understood and quantitatively explained on the basis of mathematical models. In this paper we first give an overview of the relevant experimental findings related to the swarming of *P. mirabilis*, then construct a simple model with two limit densities. We then investigate the behavior of the model as a function of the control parameters and compare it to experimental results.

**II. OVERVIEW OF EXPERIMENTAL FINDINGS****A. Differentiation**

As reviewed in Refs. [5,6], the differentiation of vegetative cells is accompanied by specific biochemical changes. Swarmer cells enhance the synthesis of flagellar proteins, extracellular polysaccharides, proteases, and virulence factors, while they exhibit reduced overall protein and nucleic acid synthesis and oxygen uptake. These findings may be explained by arguing that the production and operation of flagella is expensive and may require the repression of non-essential biosynthetic pathways. The largely (10–30 fold) elongated swarmer cells develop by a specific inhibition of cell fission which seems *not* to affect the doubling time of the cell mass or DNA.

The differentiation process is initiated by a number of external stimuli, including specific signaling molecules and physicochemical parameters of the environment. As an example of the latter, the *viscosity* of the surrounding medium is presumably sensed by the hampered rotation of the flagella [7,8]. Neither the signal molecules that initiate the differentiation nor the involved intracellular signaling pathways have

\*Email address: czirik@biol-phys.elte.hu

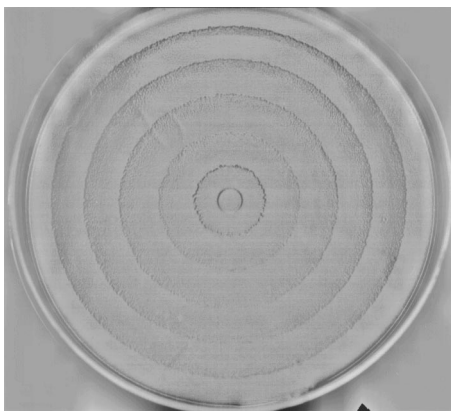


FIG. 1. Typical *Proteus mirabilis* colony. It was grown on the surface of a 2.0% agar substrate for two days. The inner diameter of the petri dish is 8.8 cm. Gray shades are proportional to the cell density: the cyclic modulation is apparent.

been identified, but a corresponding transmembrane receptor was found recently [9]. The structure of this receptor, together with other findings reviewed in Ref. [6], suggest a “quorum sensing” regulatory pathway [10], characteristic of many, cell density dependent collective bacterial behaviors like sporulation, luminescence, production of antibiotics, or virulence factors [11].

### B. Migration of swarmer cells

It is well established [5] that swarmer cell migration does not require exogenous nutrient sources, since swarmer cells replated onto media devoid of nutrients continue to migrate normally. The ability of migration depends on the local swarmer cell density as isolated single swarmer cells cannot move, while a group of them can. It was also demonstrated [12] that the mechanism by which bacteria swarm outward involved neither repulsive nor attractive chemotaxis. The typical swimming velocity (i.e., in a liquid environment) of swarmer cells is  $\approx 100$  mm/h [13] which is also their maximal swarming speed and rate of colony expansion on soft agar plates [5]. In typical experimental conditions for investigating swarming colony formation, the front advances with a speed of 0.5–10 mm/h [14,9,15,13]. Unfortunately, in these cases there is no information available on the velocity of individual swarmer cells, but it must be between the colony expansion speed and the swimming velocity.

### C. Consolidation

The molecular mechanisms of consolidation, i.e., the downregulation of the gene activity responsible for swarming behavior [16], is even less known than that of differentiation. If the swarming motility utilizes intracellular energy reserves as has been suggested [5], then swarmer cells must have a *finite lifetime*. In addition to the septation of swarmer cells taking place at the outermost terrace, inside the colony the differentiation process, i.e., the supply of fresh swarmer cells must also be shut off. The cessation of swarmer cell production does not seem to be due to severe nutrient depletion since vegetative cells keep dividing (although with de-

creasing growth rate) well inside the colony for many hours after the last swarmer cells were produced in that region [14].

### D. Colony formation

The cycle time (total length of the migration and consolidation periods) has been found [14] to be rather stable ( $\approx 4$  h) for a wide range of nutrient and agar content of the medium. The size of the terraces and the duration of the migration phases were strongly influenced (up to an order of magnitude, and up to a factor of 3, respectively) by the agar hardness. The nutrient concentration did not have an observable effect on these quantities from 0.01% up to 1% glucose concentrations. There was, however a remarkable positive correlation between the cycle time and the doubling time (ranging from 0.7 up to 1.8 h) of the cells.

Two interfacing colonies inoculated with a time difference of a few hours, and therefore being in different phases of the migration-consolidation cycle, were found to maintain their characteristic phases [14,15]. Thus, the control of the swarming cycle must be sufficiently local.

### E. Cycle rescheduling

A few experiments investigated the cell density dependence of the duration of quiescent growth (*lag phase*) prior to the first migration phase. These studies clearly revealed that vegetative cells have to reach a threshold density to initiate swarming [14,15], in accord with the suggested quorum sensing molecular pathway of the initiation of swarmer cell differentiation.

Agar cutting experiments demonstrated that a cut inside the inner terraces does not influence the swarming activity [15]. However, when the cut was made just behind the swarming front, the duration of the swarming phase was shortened and consolidation was lengthened by up to 40% [15].

Even more interestingly, *mechanical mixing* of the cell populations before the expected beginning of consolidation expands the duration of the swarming phase considerably, by up to 50% [13]. This finding, together with *replicaprinting* experiments [13] demonstrates that at the beginning of the consolidation phase a large pool of swarmer cells still exists, and seems to be “trapped” at the rear of the outermost terrace.

## III. MODEL

Taking into account the above described experimental findings, here we construct a model which is capable of explaining most of the observed features of colony expansion through swarming cycles.

(i) The model is based on vegetative and swarmer cell population densities *only*, denoted by  $\rho^0$  and  $\rho^*$ , respectively. These values are defined on the basis of cell mass instead of cell number; therefore, one unit of swarmer cells is transformed into one unit of vegetative cells during consolidation.

(ii) Vegetative cells grow and divide with a constant rate

$r_0 \approx 1 \text{ h}^{-1}$  [14,15]. This will later allow us to establish a direct correspondence between cell density increase and elapsed time.

(iii) Usually, swarmer cell differentiation is initiated when the local density of the vegetative cells exceeds a threshold value ( $\rho_{min}^0 \approx 10^{-2} \text{ cells}/\mu\text{m}^2$  [14,15]). (Before the beginning of the first swarming phase, experiments indicated the presence of an extra time period  $t_l$  which is probably associated with the biochemical changes required to develop the ability of the swarming transition. This effect is present only at the seeding of the colony, thus  $t_l=0$  otherwise.) When  $\rho^0 = \rho_{min}^0$  at time  $t_0$ , some of the vegetative cells enter the differentiation process, modeled by introducing a rate  $r$ . Since the biomass production rate is assumed to be unchanged during the differentiation process, the rate of producing new vegetative cells is  $r_0 - r$ , and the differentiating cells elongate with the normal growth rate  $r_0$ .

(iv) The full development of swarmer cells, i.e., a typical 20-fold increase in length needs a time ( $t_d \approx \ln 20/r_0 \approx 3 \text{ h}$ ) comparable with, or even longer than the length of a consolidation period, hence cannot be neglected. Therefore, the first ‘‘real’’ swarmer cells, which are able to move appear only at  $t_0 + t_d$ .

(v) The production of swarmer cells is limited in time, and the length  $\tau$  of the time interval during which vegetative cells can enter the differentiation process is another phenomenological parameter of our model. As here we focus on the periodicity of colony expansion, we do not consider what happens in densely populated regions after  $t_0 + \tau$ . Specifically, in our model any activity of the vegetative cells ceases in these parts of the system.

(vi) Swarmer cells can migrate only if their density exceeds a threshold density  $\rho_{min}^*$ . Above this threshold, swarmer cells are assumed to move randomly with a diffusion constant  $D_0$ . Both of these parameters are thought to be determined by the quality of the agar substrate. The finite lifetime of swarmer cells is incorporated into the model through a constant rate ( $r^*$ ) decay.

Unfortunately there are no good estimates on these parameters in the literature. According to recent experimental observations [17],  $\rho_{min}^*$  is less than 10% of the value of  $\rho^0$  prior to the beginning of the swarming phase, i.e.,  $0.1\rho_{min}^0 e^{r_0 t_d} \approx 10^{-2} \text{ cells}/\mu\text{m}^2$ .  $D_0$  may be estimated as  $v_0^2 t_p/2$  with  $v_0$  being the typical speed of swarming cells and  $t_p$  being the persistence time of their motion. As  $v_0$  is approximately 30 mm/h (see Sec II B) and  $t_p$  is in the order of minutes,  $D_0$  is estimated to be in the order of  $10 \text{ mm}^2/\text{h}$ .

The above considerations lead to the set of equations

$$\begin{aligned} \dot{\rho}^0(t) &= r_0 \rho^0(t) + \Gamma(t) - \Gamma^*(t), \\ \dot{\rho}^*(t) &= -\Gamma(t) + \Gamma^*(t - t_d) e^{r_0 t_d} + \nabla D(\rho^*) \nabla \rho^*, \end{aligned} \quad (1)$$

where the consolidation ( $\Gamma$ ) and differentiation ( $\Gamma^*$ ) terms are given by

$$\Gamma = r^* \rho^* \quad \text{and} \quad \Gamma^* = r(\rho^0, t) \rho^0. \quad (2)$$

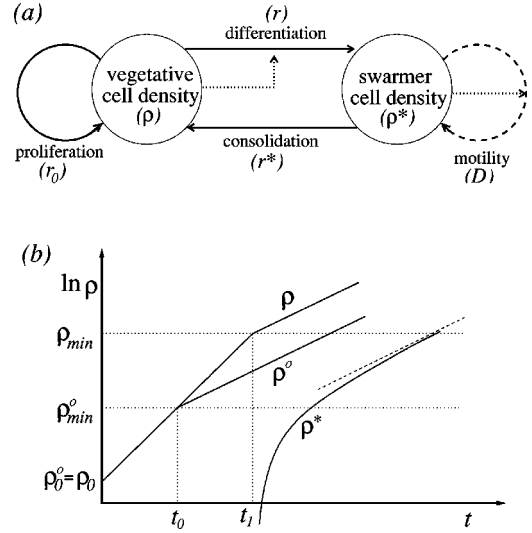


FIG. 2. Schematic representation of the model for swarming colony formation. (a) The two basic quantities are the vegetative and swarmer cell densities, which can be transformed into each other, and changed by proliferation and motility. The dotted lines represent regulatory (threshold) effects: The rate of differentiation is assumed to be dependent on the vegetative cell density, and the motility of swarmer cells is also determined by their local density. (b) Notations and typical time courses of vegetative and swarmer cell densities prior to the beginning of the first migration phase. If  $t < t_0$ , the density  $\rho$  (or  $\rho^0$ ) grows at a constant rate  $r_0$ . After reaching the density threshold  $\rho_{min}^0$ , vegetative cells keep growing only with a rate  $r_0 - r$ , but the total density ( $\rho$ ) of the vegetative cells and the differentiating swarmer cells continues to grow with a rate  $r_0$ . After the time required for the full elongation of a swarmer cell (when  $\rho$  reaches  $\rho_{min}$ ),  $\rho^*$  becomes positive, and for  $r^*=0$  would grow asymptotically with a rate  $r$ .

Equations (1) can be significantly further simplified by making use of the possibility to measure elapsed time with the increase in  $\rho^0$ . In particular, neglecting correction terms related to consolidation in areas where  $\rho^0 > \rho_{min}^0$ , i.e., where primarily differentiation takes place, we can cast  $\Gamma^*(t - t_d) e^{r_0 t_d}$  in the form

$$\begin{aligned} r \rho^0(t - t_d) e^{r_0 t_d} &= r \rho_{min}^0 e^{(r_0 - r)(t - t_d - t_0)} e^{r_0 t_d} \\ &= r \rho_{min}^0 e^{r_0(t - t_0)} e^{-r(t - t_0 - t_d)} = r \rho^0(t) e^{r t_d} \end{aligned} \quad (3)$$

for  $t > t_0 + t_d \equiv t_1$ . Let us introduce a transformed population density  $\rho$  as

$$\rho(t) = \begin{cases} \rho^0(t) & \text{for } \rho^0 < \rho_{min}^0, \text{ i.e., for } t < t_0 \\ \rho^0(t) e^{r(t - t_0)} & \text{for } \rho^0 > \rho_{min}^0 \text{ and } t < t_1 \\ \rho^0(t) e^{r t_d} & \text{for } \rho^0 > \rho_{min}^0 \text{ and } t > t_1, \end{cases} \quad (4)$$

which is in fact the total density of the vegetative and the differentiating, but not yet fully differentiated swarmer cells (see Fig. 2). With this notation, using Eq. (3) and similar

considerations for  $t_0 < t < t_0 + t_d$ , Eqs. (1) can be written into simple, not retarded forms

$$\begin{aligned}\dot{\rho} &= r_0\rho + r^*\rho^* - r(\rho)\rho, \\ \dot{\rho}^* &= -r^*\rho^* + r(\rho)\rho + \nabla D(\rho^*)\nabla\rho^*,\end{aligned}\quad (5)$$

where

$$r(\rho) = \begin{cases} r & \text{for } \rho_{min} < \rho < \rho_{max} \\ 0 & \text{otherwise,} \end{cases} \quad (6)$$

with  $\rho_{min} = e^{r_0 t_d} \rho_{min}^0 \approx 10^{-1}$  cells/ $\mu\text{m}^2$  and  $\rho_{max}(\tau) = e^{(r_0 - r)\tau} \rho_{min}$ . Thus  $\tau$  and  $\rho_{max}$  mutually dermine each other. If the  $\Gamma \ll (r_0 - r)\rho$  condition does not hold in the  $[t_0, t_1]$  time interval, then  $\rho_{min}$  must also be treated as a dynamical variable. This case will not be considered here. In the following we use  $\rho$  for the characterization of vegetative cell density, and  $\rho_{max}$  instead of  $\tau$ .

## IV. RESULTS

### A. Numerical method in one dimension

The model defined through Eqs. (5) has the following seven parameters: the rates  $r_0$ ,  $r$ , and  $r^*$ ; threshold densities  $\rho_{min}$ ,  $\rho_{max}$  (or  $\tau$ ), and  $\rho_{min}^*$ ; and diffusivity  $D_0$ . However, this number can be reduced to four by casting the equations in a dimensionless form using  $1/r_0 \approx 1$  h as time unit,  $\rho_{min} \approx 0.1$  cells/ $\mu\text{m}^2$  as density unit and  $x_0 = \sqrt{D_0/r_0} \approx 3$  mm as the unit length. The resulting control parameters are  $r/r_0$ ,  $r^*/r_0$ ,  $\rho_{max}/\rho_{min} = \exp[(r_0 - r)\tau]$ , and  $\rho_{min}^*/\rho_{min}$ . To obtain continuous density profiles, the step-function dependence of  $D$  on  $\rho^*$  was replaced by

$$D(\rho^*) = \frac{D_0}{2} \left[ 1 + \tanh 2\alpha \frac{\rho^* - \rho_{min}^*}{\rho_{min}^*} \right], \quad (7)$$

with  $\alpha = 10$  providing a rather steep, but continuous crossover. The following results do not depend on the particular choice of Eq. (7).

Representative examples of the time development of the model are shown in Fig. 3. The production of swarmer cells is localized, and determined by the density profile of vegetative cells at the end of migration periods. In this particular model  $\rho(x)$  is decreasing toward the colony edge; therefore, in the migration phases the source of swarmer cells is moving outward. The front of swarmer cells is expanding from the inside of the last terrace. Because of the decay term  $\Gamma$ , cells become nonmotile first at the colony edge.

### B. Phase diagram

Each of the dimensionless control parameters can have an important effect on the dynamics of the system. As an example, if the duration  $\tau$  of swarmer cell production is increased, then the consecutive swarming cycles are not separated and a continuous expansion takes place with damped oscillations [Fig. 3(b)]. To map the behavior of the system as a function of the control parameters, the following procedure

was applied. Migration periods were identified by requiring  $\max_x \rho^*(x) > \rho_{min}^*$ . For a given set of parameters we determined the lengths  $\{t_i\}$  of the consecutive migration periods, and the system was classified as *periodic* if the three largest values of the set  $\{t_i\}$  were the same within 20%. Otherwise, the expansion was classified as *continuous* as long as  $\max_i \{t_i\}$  was large enough: comparable with the total duration of the simulated expansion.

The behavior of the model is summarized in Fig. 4, where the boundaries of the various regimes are plotted for three different values of  $r^*/r_0$ . We found, that  $r$  and  $\rho_{max}$  can be combined into one relevant parameter, the swarmer cell production density, as

$$P = \int_{-\infty}^{\infty} \Gamma^*(x, t) dt = \frac{r}{r_0 - r} (\rho_{max} - \rho_{min}), \quad (8)$$

which quantity does not depend on the choice of position  $x$ . As the inset demonstrates, for a given  $P$ , the actual values of  $r$  or  $\rho_{max}$  are irrelevant to this kind of classification in the parameter regime investigated. The general structure of the phase diagram was found to be similar for various values of  $r^*$ . For large enough  $P$  or low enough  $\rho_{min}^*$  a continuous expansion takes place, while for too small  $P$  or large  $\rho_{min}^*$  the expansion of the system is finite. For intermediate values of these parameters an oscillating growth develops, exhibiting very distinguishable consolidation and migration phases. As the lifetime of the swarmer cells is increased, the parameter regime, in which periodic behavior is exhibited, shrinks and is moved toward lower  $P$  values.

One can easily estimate the position of the boundary of the nongrowing phase based on that (i) the width  $w$  of the terraces is small (this assumption is justified later, in Fig. 7); thus (ii) the time required for the diffusive expansion of the swarmer cells is much shorter than their lifetime, which, in turn, is (iii) shorter than the duration of a swarming cycle:  $r^*/r_0 \sim 1$ . The amount of swarmer cells produced in one period is  $Pw$ . Neglecting the decay during expansion, the width  $w'$  of the next, new terrace can be determined from the conservation of cell number as

$$2\rho_{min}^* w' = w(P + \rho_r^* - \rho_{min}^*), \quad (9)$$

where  $\rho_r^*$  denotes the swarmer cell density remaining from the previous swarming cycle and the symmetric expansion of the released swarmer was also taken into account. To achieve a sustainable growth  $w' \geq w$  is required, resulting in a condition  $3\rho_{min}^* \leq P + \rho_r^*$ . If  $\rho_r^* \ll P$ , as one can expect for  $r^*/r_0 \sim 1$ , for the boundary of the nongrowing phase we obtain

$$P = 3\rho_{min}^*, \quad (10)$$

which, as Fig. 4 demonstrates, is indeed in good agreement with the numerical data.

### C. Terrace formation

The average length  $T$  of a full swarming cycle was calculated by determining the position of the peak in the power

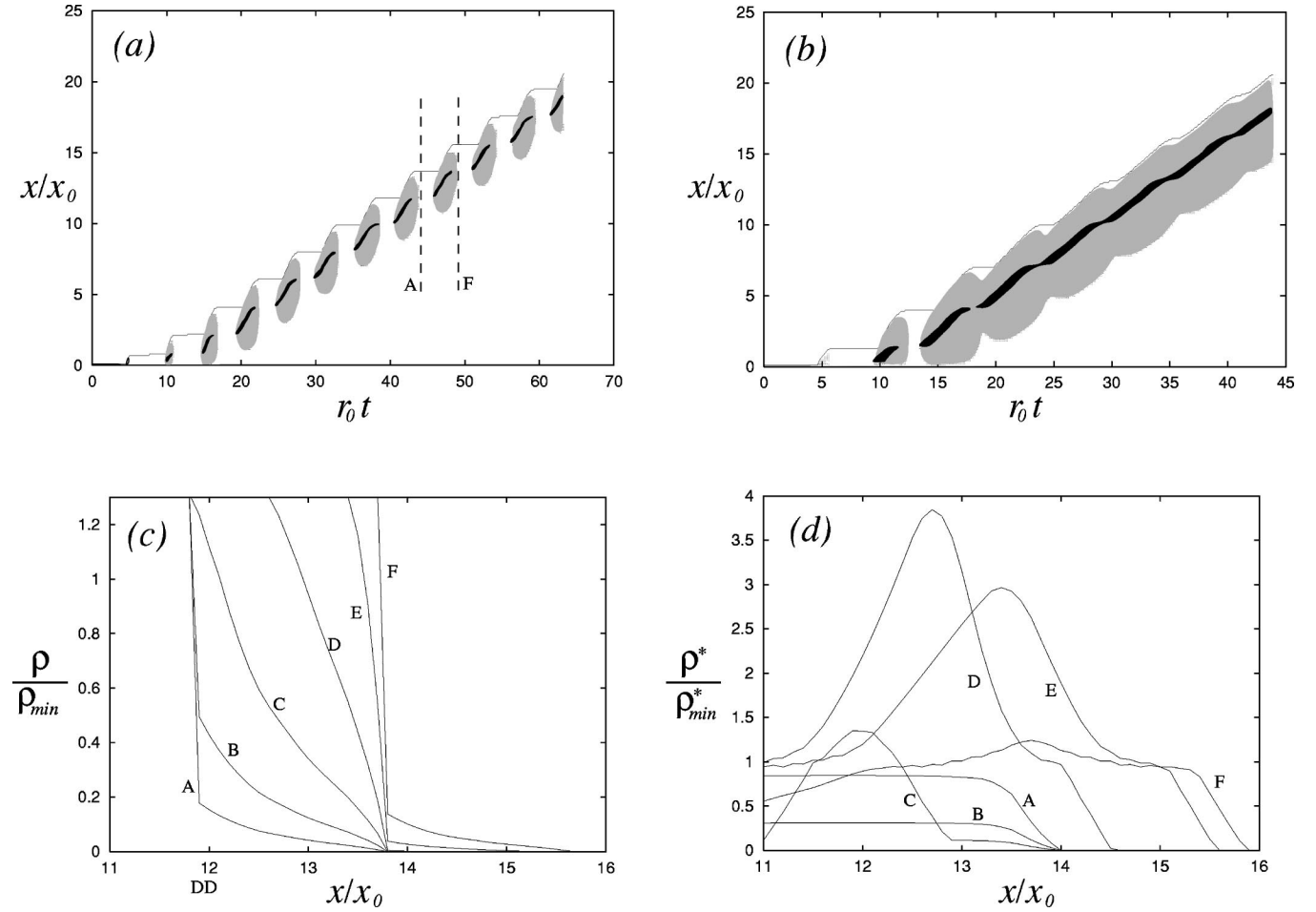


FIG. 3. Time development of the model obtained by numerical integration of the equations, starting from a localized “inoculum” at  $t = 0$  and  $x = 0$ . The continuous line represent the colony boundary [maximal value of  $x$  for which  $\rho(x) + \rho^*(x) > 0$ ]. The filled gray and black areas are regions where swarmer cells are motile, and where swarmer cells are produced, respectively. For  $\rho_{max} = 1.3$ ,  $\rho_{min}^* = 0.01$ ,  $r = 0.3$ , and  $r^* = 1.0$ , the expansion of the system is clearly periodic (a). If we increase the production of swarmer cells by increasing  $\rho_{max}$  to 2.0 then the periodicity is gradually lost and a continuous expansion takes place (b). The density profiles of the vegetative and swarmer cell populations are plotted for consecutive time points in (c) and (d), respectively. Curves A–F correspond to  $r_0 t = 44, 45, \dots, 49$ , i.e., a complete swarming cycle.

spectrum of  $S(t) = \int_0^\infty \rho^*(x, t) dx$ , the time dependence of the total number of swarmer cells in the system. As Fig. 5 demonstrates, the dimensionless cycle time values are widely spread between values of 3 and 12. However,  $T$  is *only* sensitive to changes in  $r_0$ ,  $r^*$ , and  $\rho_{min}^*/\rho_{min}$ ; hence it does not depend on  $\rho_{max}$  or  $\tau$ .

The average expansion speed  $v$  and terrace size  $w$  were also calculated in the parameter regime resulting oscillatory expansion of the colony. First we determined the time  $t_{1/3}$  when the system reached one-third its maximal simulated expansion  $R_{max} = R(t_{max})$ , with  $R(t)$  being the position of the expanding colony edge and  $t_{max}$  is the total duration of the simulation. The average speed was then calculated for the time interval between  $t_{min} = \max(t_{1/3}, t_{max} - 5T)$  and  $t_{max}$ : for the last  $5T$  long time interval, or for the last two-thirds of the total expansion, depending on which was smaller. After obtaining  $v$  as  $[R_{max} - R(t_{min})]/(t_{max} - t_{min})$ , the average terrace width was calculated as  $w = vT$ . Figure 6 shows the dependence of these parameters on the swarmer cell produc-

tion density  $P$  and migration density threshold  $\rho_{min}^*$ . In general, decreasing  $\rho_{min}^*$  or increasing  $P$  results in an increase in both  $w$  and  $v$ . As Fig. 7 demonstrates, for a given  $r^*$ , the relevant parameter controlling  $w$  is  $P/\rho_{min}^*$ .

The results on the cycle time  $T$  (Fig. 5) can be interpreted as follows. As  $\rho_{min}^*$  is a good estimate on the density of swarmer cells in the expanding front, at the end of migration phase the vegetative cell density within the new terrace is given by  $r^* \rho_{min}^* T^*$ , with  $T^*$  being the duration of the migration phase. Now the length of the consolidation phase,  $T - T^*$ , is determined by the requirement that  $\rho$  must reach  $\rho_{min}$ :

$$\rho_{min} = r^* \rho_{min}^* T^* e^{r_0(T-T^*)} = r^* \rho_{min}^* \frac{T^*}{e^{r_0 T^*}} e^{r_0 T}. \quad (11)$$

As  $T^* \approx 1/r_0$ , estimate (11) is simplified to

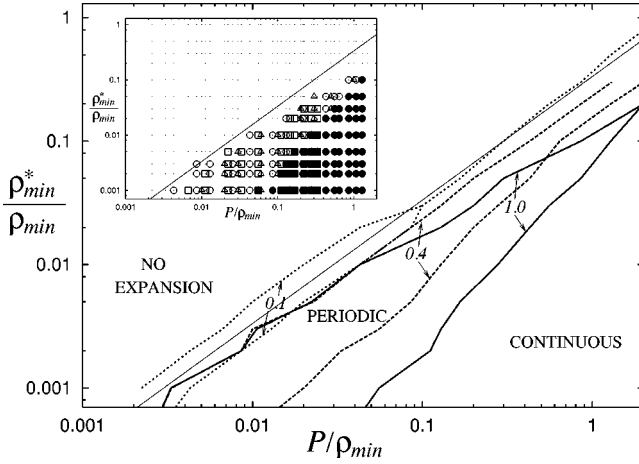


FIG. 4. Phase diagram of the system as the function of cumulative swarmer cell production density  $P$  and migration threshold  $\rho_{min}^*$  for various values of swarmer cell decay rate  $r^*$ . If the production is high enough or the motility threshold is low enough, then continuous expansion can be observed. On the other hand, if the production is too low or the motility threshold is too high, then no expansion takes place. In an intermediate regime periodic growth can be observed. The boundaries of this parameter regime are plotted for  $r^*/r_0 = 1.0$  (thick continuous line),  $0.4$  (thick dashed line), and  $0.1$  (thick dotted line). The thin continuous line represents an approximate upper bound (10) for cyclic colony expansion. The inset demonstrates that the fourth parameter of the model,  $r$ , is irrelevant: for  $r^*/r_0 = 1$  and  $r/r_0 = 0.01$  ( $\square$ ),  $0.3$  ( $\circ$ ),  $0.5$  ( $\triangle$ ) and various values of  $\rho_{max}$  and  $\rho_{min}^*$  the type of colony expansion was classified. Open symbols correspond to cyclic growth, filled symbols correspond to continuous growth, and dots denote no expansion. Note that the corresponding regions completely overlap irrespective of the value of  $r$ .

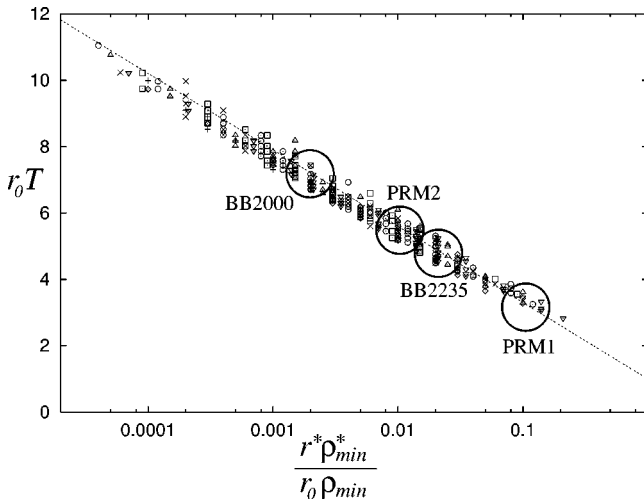


FIG. 5. The cycle time  $T$  as a function of the approximate consolidation rate  $r^* \rho_{min}^*$ . The data collapse indicates that the impact on  $T$  of the other parameters ( $\rho_{max}$  and  $r$ ) is negligible. The various symbols correspond to different values of  $r^*/r_0$  as 0.1 (+), 0.2 ( $\times$ ), 0.3 ( $\square$ ), 0.4 ( $\circ$ ), 0.5 ( $\triangle$ ), 0.7 ( $\nabla$ ), and 1.0 ( $\diamond$ ). The dashed line is a plot of Eq. (12). Circles mark out the assumed parameter values characteristic of four different *P. mirabilis* strains.

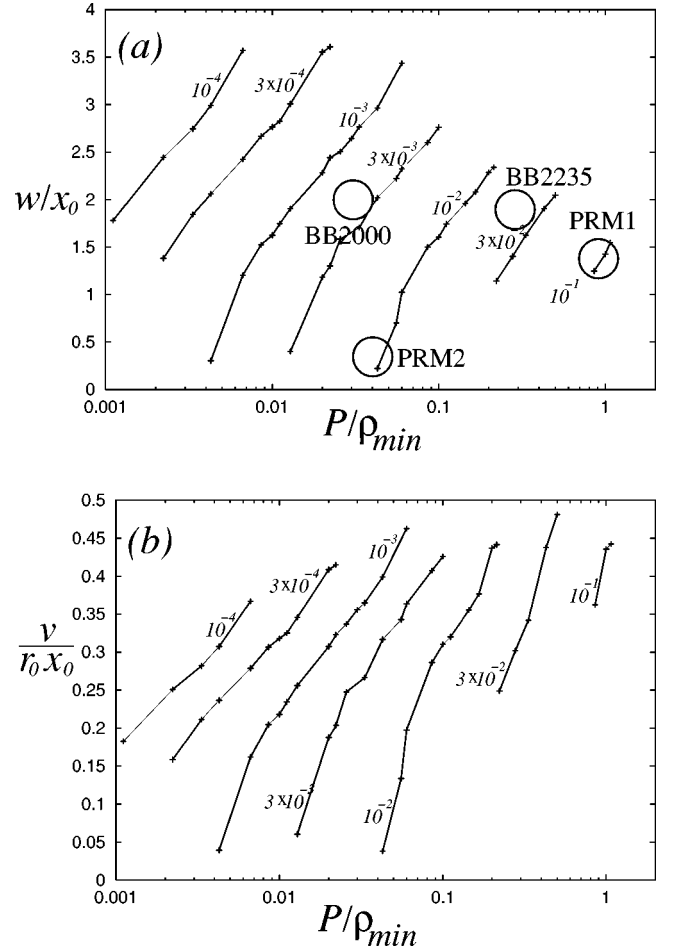


FIG. 6. Terrace size (a) and expansion speed (b) of the system for  $r^*/r_0 = 1$  as a function of the dimensionless swarmer cell production density  $P$ . The connected points correspond to various values of the migration threshold  $\rho_{min}^*/\rho_{min}$ . In general, decreasing  $\rho_{min}^*$  or increasing  $P$  results in an increase in both  $w$  and  $v$ . Only parameters resulting in periodic expansion were investigated. Circles mark out the assumed parameter values characteristic of four different *P. mirabilis* strains.

$$r_0 T = \ln \frac{r_0 \rho_{min} e}{r^* \rho_{min}^*}, \quad (12)$$

which gives a rather accurate fit to the numerically determined data (Fig. 5).

#### D. Lag phase

Since the duration ( $T_L$ ) of the lag phase (the time period before the first migration phase) has been in the focus of many recent experiments, we now turn our attention toward this quantity. At least four processes determine  $T_L$ . First, there is a time  $t_l$  associated with the biochemical changes required to switch into swarming mode. As discussed in Sec. II A, these processes take place only prior the first swarming phase, and are presumably related to sensing the altered environmental conditions. Second, the cell population must reach the threshold density  $\rho_{min}^0$  (at time  $t_0$ ). Third,  $t_d$  time is

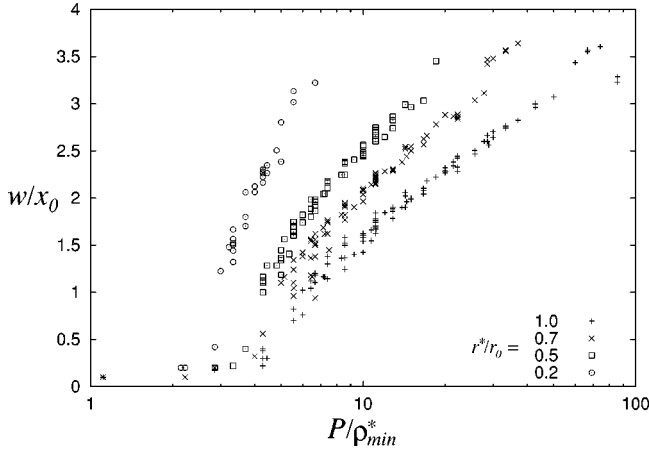


FIG. 7. Terrace size  $w$  vs  $P/\rho_{min}^*$  for various values of  $r^*/r_0$ . Note the collapse of the data presented in Fig. 6(a). The terrace size vanishes approaching the parameter regime where no sustainable expansion of the system is possible.

required to produce fully differentiated swarmer cells (at time  $t_1$ ). Finally, the density of the swarmer cells must reach the migration threshold  $\rho_{min}^*$ . Let us investigate how these parameters depend on the initial inoculum density  $\rho_0$ .

As  $\rho$  grows with a rate  $r_0$  until the appearance of swarmer cells,

$$r_0 t_1 = \max[t_l + t_d, \ln(\rho_{min}/\rho_0)]. \quad (13)$$

The time development of  $\rho^*$  can be estimated by the integration of Eq. (5) with  $r^*=0$  (i.e., assuming  $\Gamma \ll \Gamma^*$ ), yielding

$$\rho^*(t+t_1) = \frac{r}{r_0 - r} \rho_0 e^{r_0 t_1} [e^{(r_0 - r)t} - 1]. \quad (14)$$

Therefore,  $t^* = T_L - t_1$  is given by

$$r_0 t^* = \frac{1}{1 - r/r_0} \ln \left( \frac{r_0 - r}{r} \frac{\rho_{min}^*}{\rho_0 e^{r_0 t_1}} + 1 \right), \quad (15)$$

an expression usually giving a minor correction to  $t_1$ .

Figure 8(a) shows the above calculated  $r_0 T_L$  vs  $\rho_0$  for  $t_l = 0$ . The increase in length of the swarmer cells was assumed to be 20-fold; thus  $r_0 t_d = \ln 20 \approx 3$ , which value can be seen for  $\rho_0 \gg \rho_{min}$ . In the opposite limit, when  $\rho_0 \ll \rho_{min}$ , we have  $r_0 T_L \approx -\ln \rho_0 + \text{const}$ . These relations allow the determination of both  $r_0$  and  $r$  (using the known value of  $\rho_{min}^*/\rho_{min}$ ) from the experimental data on  $T_L(\rho_0)$ .

### E. Comparison with experiments

Most of the published experimental data are related to the average period length  $T$  and terrace size  $w$ . From these parameters the average expansion speed can be calculated as  $v = w/T$ , i.e.,  $v$  is not an independent quantity. As we saw in Sec. IV D, from the density dependence of the lag phase the parameters  $r_0$ ,  $t_l + t_d$ , and  $r$  can be estimated. Note that this estimate on  $r_0$  is in principle different from the value ob-

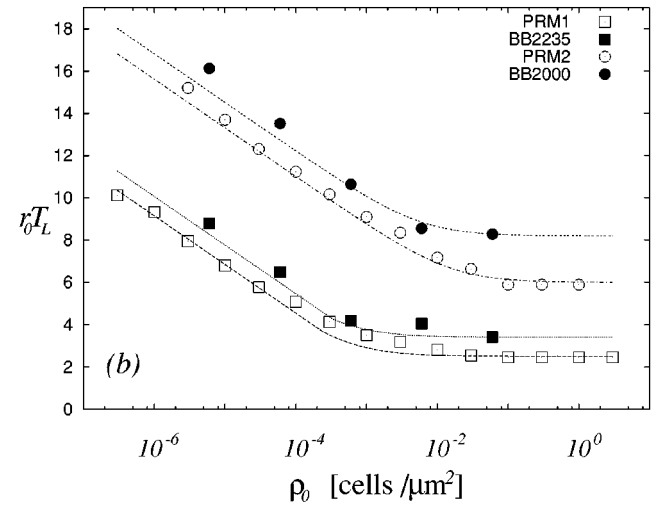
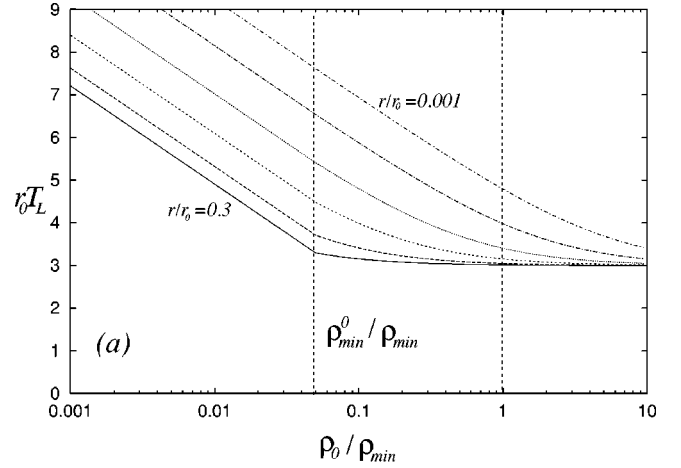


FIG. 8. (a) Length  $T_L$  of the lag phase vs the initial inoculum density  $\rho_0$  for  $t_l = 0$ ,  $r_0 t_d = 3$ , and various values of  $r/r_0$  (0.3, 0.1, 0.03, 0.01, 0.003, and 0.001). The transition between the regimes separated by  $\rho_{min}^0$  becomes more smooth for decreasing  $r/r_0$ . (b) The experimentally calculated  $r_0 T_L$  values vs the estimated inoculum density (based on 5 and 7-mm inoculum droplet sizes for the RPM and BB strains, respectively) and the corresponding fits using Eqs. (13) and (15).

tained by the usual methods based on densitometry in liquid cultures. Technically,  $\rho_{min}^*$  could be also determined [14], but such measurements are not yet published.

There are four *Proteus* strains studied systematically in experiments: the PRM1, PRM2, BB2000, and BB2235 strains (see Table I). To extract the values of the model's parameters the following procedure was applied. (i) We estimated  $r_0$  based on lag phase length measurements. (ii) From the calculated  $r_0 T$  values the  $\rho_{min}^*/\rho_{min}$  ratio was estimated (assuming  $r^*/r_0 = 1$ ) based on Eq. (12); see Fig. 5. (iii) Using Eqs. (14) and (15), by a nonlinear fitting procedure [Levenberg-Marquardt method [18]; see Fig. 8(b)],  $\rho_{min}$ ,  $r$ , and  $t_l + t_d$  were determined. (The latter value is not relevant in respect the periodicity of the behavior.) (iv) Knowing  $\rho_{min}^*$  and  $\rho_{min}$ , from the experimental terrace width data  $x_0$  and  $P$  can be estimated using Fig. 6. (v) Finally,  $\tau$  is given by

TABLE I. Summary of experimental data for four different *P. mirabilis* strains under various experimental conditions. The value of  $r_0$  was determined from growth monitoring in liquid cultures.

Strain		PRM1		PRM2	BB2000	BB2235			
Experimental condition	Temperature	32 °C	32 °C	32 °C	37 °C	22 °C	32 °C	37 °C	37 °C
	Agar	2.0%	2.45%	2.0%	n.a.	n.a.	2.0%	n.a.	n.a.
	Reference	[14]	[14]	[15]	[14]	[14]	[14]	[9]	[9]
Colony level	$T$ (h)	4.7	4.7	4.0	3.5	8.5	6.0	3.0	3.1
	$v$ (mm/h)	1.7	0.6	1.0	n.a.	n.a.	n.a.	3.3	3.3
	$w$ (mm)	8.0	3.0	3.8	n.a.	n.a.	n.a.	10	10
Cellular level	$r_0$ (1/h)	0.6	0.6	n.a.	1.0	0.4	n.a.	n.a.	n.a.

$$r_0 \tau = \ln \left( \frac{Pr_0}{\rho_{min} r} + 1 \right). \quad (16)$$

The parameter values of the model are summarized in Table II, together with the predictions on  $T$ ,  $v$ , and  $w$ . An excellent agreement can be achieved with biologically relevant parameter values.

Two classes of model parameters should be distinguished: (a) those which are related to the growth and differentiation of the cells [ $r_0$ ,  $r^*$ ,  $\rho_{min}$ , and  $P(r, \tau)$ ], and (b) those which depend on agar softness ( $D_0$  and  $\rho_{min}^*$ ). For a given strain we expect that a change in the agar concentration influences

only the latter group, while changes in temperature may affect both, but primarily  $r_0$ . In fact, as Table II demonstrates, by changing  $D_0$  and keeping all the other, growth-related parameters constant, we could *quantitatively* reproduce the colony behavior observed on various agar concentrations. A similar statement holds for the temperature effects as well, where the only parameter we changed was the growth rate  $r_0$ .

## V. DISCUSSION

Periodic bacterial growth patterns have been in the focus of research in the last few years. Since a colony can be

TABLE II. Model parameters and the corresponding results for the strains and experimental conditions specified in Table I. The model has seven microscopic parameters, the rates  $r_0$ ,  $r$ , and  $r^*$ , the threshold densities  $\rho_{min}$ ,  $\rho_{min}^*$ , and  $\rho_{max}$ , and the diffusivity  $D_0$ . For each of the strains  $r^* = r_0$  was assumed. For comparison, other (derived) microscopic parameters are also included. The calculated period lengths, terrace sizes, and expansion speeds are also presented together with the corresponding experimental values (in parentheses). The values marked by an asterisk (\*) were derived from the lag phase length data based on Eqs. (13) and (15). Note the similarity between the PRM1 and BB2235, and also between the PRM2 and BB2000 strains.

Strain		PRM1		PRM2	BB2000	BB2235			
Experimental condition	Temperature	32 °C	32 °C	32 °C	37 °C	22 °C	32 °C	37 °C	37 °C
	Agar	2.0%	2.45%	2.0%	n.a.	n.a.	2.0%	n.a.	n.a.
	$r_0$ (1/h)	0.53* (0.6)	0.53* (0.6)	0.7*	1.0	0.4	1.0*	2.5*	1.5*
Microscopic parameters (independent)	$\rho_{min}$ (cell/ $\mu\text{m}^2$ )			0.06			0.6	2.0	0.2
	$\rho_{min}^*$ (cell/ $\mu\text{m}^2$ )			$6 \times 10^{-3}$			$6 \times 10^{-3}$	$4 \times 10^{-3}$	$4 \times 10^{-3}$
	$\rho_{max}$ (cell/ $\mu\text{m}^2$ )			0.6			240	3000	2.2
	$r/r_0$			$10^{-1}$			$10^{-4}$	$2 \times 10^{-5}$	$3 \times 10^{-2}$
	$D_0$ (mm <sup>2</sup> /h)	20	3.2	6	–	–	–	60	40
(derived)	$\rho_{min}^0$ (cell/ $\mu\text{m}^2$ )			$3 \times 10^{-3}$			$3 \times 10^{-2}$	$10^{-1}$	$10^{-2}$
	$P/\rho_{min}$			0.9			0.04	0.03	0.3
	$\tau/T$			0.7			0.9	0.9	0.3
	$\rho_{min}^*/\rho_{min}$			$10^{-1}$			$10^{-2}$	$2 \times 10^{-3}$	$2 \times 10^{-2}$
	$x_0$ (mm)	6	2.3	3.0	–	–	–	5.0	5.0
	$v_0$ (mm/h)	50	20	27	–	–	–	85	70
Macroscopic behavior	$T$ (h)	5.5 (4.7)	5.5 (4.7)	4.7 (4.0)	3.3 (3.5)	8.2 (8.5)	5.6 (6.0)	2.9 (3.0)	3.2 (3.1)
	$v$ (mm/h)	1.4 (1.7)	0.5 (0.6)	0.8 (1.0)	n.a.	n.a.	n.a.	3.4 (3.3)	3.1 (3.3)
	$w$ (mm)	7.8 (8.0)	3.0 (3.0)	3.9 (3.8)	n.a.	n.a.	n.a.	10 (10)	10 (10)

viewed as a system where diffusing nutrients are converted into diffusing bacteria, one may not be surprised by the emergence of spatial structures [19]. However, the periodic patterns of bacterial colonies are qualitatively different from the Liesegang rings (for a recent review, see Ref. [20]) developing in reaction-diffusion systems: the spacing between the densely populated areas is uniform and independent of the concentration of the other diffusing species, i.e., the nutrients. The Turing instability is also well known for producing spatial structures [21], but in this case the pattern emerges simultaneously in the whole system. It is also known that bacteria can aggregate in steady concentric ring structures as a consequence of chemotactic interactions [22,23], but, as discussed in Sec. II., it is established that swarming of *P. mirabilis* does not involve chemotaxis communication. Therefore, none of the well known generic pattern forming schemes can explain the colony structure of swarming bacteria.

As we mentioned in Sec. I, oscillatory growth is also exhibited by other bacterial species. One of these, *Bacillus subtilis*, has been the subject of systematic studies on colony formation, and a number of models have been constructed to explain the observed morphology diagram (for recent reviews, see Refs. [24,25]). Only one model addressed the problem of migration and consolidation phases: Mimura *et al.* [26] set up a reaction-diffusion system in which the decay rate of the bacteria was dependent both on their concentration and the locally available amount of nutrients. The periodic behavior is then a consequence of the following cycle: if nutrients are used up locally, then the bacterial density starts to decay, preventing the further expansion of the colony. Nutrients diffuse to the colony and accumulate due to the reduced consumption of the already decreased population. The increased nutrient concentration gradually allows an increase in population density and an expansion of the colony, which starts the cycle from the beginning. While this can be a sound explanation for *B. subtilis*, as we discussed in Sec. II, the nutrient limitation clearly cannot explain neither the differentiation nor the consolidation of *P. mirabilis* swarmer cells.

Another recent study [27] focused on the swarming of *Serratia liquefaciens*. In this case the structure of the molecular feedback loops are better explored, and were resolved in the model. The production of a wetting agent was initiated by high concentrations of specific signalling molecules. The colony expansion was considered to be a direct consequence of the flow of the wetting fluid film, in which process the only effect of bacteria (besides the aforementioned production) was changing the effective viscosity of the fluid. The wetting agent production was downregulated through a negative feedback loop involving swarmer cell differentiation. This scenario is certainly not applicable to *P. mirabilis*, where swarmer cells actively migrate outward and their role is quite the opposite: enhancing the expansion of the colony.

The first theoretical analysis focusing on *P. mirabilis* was performed by Esipov and Shapiro (ES) in Ref. [28]. Their model was constructed based on assumptions similar to ours, and could reproduce the alternating migration and consolidation phases during the colony expansion. However, the com-

plexity of the ES model involves a rather large number of model parameters, which practically impedes both the full mapping of the parameter space and a quantitative comparison of the model results with experimental findings. The major differences between our model and ES's can be summarized as follows: (i) We do not resolve the *age* of the swarmer population. Instead, we have a density measure and a constant decay rate, implying an exponential lifetime distribution on the (unresolved) level of individual cells. Since the available microbiological observations [5,13] suggest *only* that the lifetime is finite, there is no reason for preferring any specific distribution. (ii) We did not incorporate into our model an unspecified "memory field" with a *built-in hysteresis*. Instead, we implemented a *density-dependent motility* of the swarmer cells, which behavior was indeed observed [4–6]. (iii) In our model the fully differentiated swarmer cells *do not grow*, which assumption is probably not fundamental for the reported behavior, but it seems to be more realistic because of the repression of many biosynthetic pathways [5]. (iv) Finally, we do not consider any specific *interaction between the motility of swarmer cells and the non-motile vegetative cell population*. Although such interactions probably exist, they are undocumented, and as we demonstrated, are not required for the formation of periodic swarming cycles. However, such effects can be important in the actual determination of the density profiles.

With these differences, which are not compromising the biological relevance of the model, we were able to map the phase diagram *completely*, establish approximate analytical formulas, and estimate the value of *all* model parameters in the case of four different strains. In addition, experimental data measured under various conditions could be explained with one particular parameter setting in the case of the PRM1 strain, indicating the predictive power of our approach. Our model is a *minimal* model in the sense that all of the explicitly considered effects (thresholds, diffusion, etc.) were required to produce the oscillatory behavior; thus it cannot be simplified further. Such minimal models can serve as a comparison baseline for later investigations of various specific interactions.

The values of the microscopic parameters of the model can be either measured directly (like  $r_0$ ,  $\rho_{min}^*$ ,  $\rho_{min}$ ,  $\rho_{max}$ , or  $r^*$ ) or can be determined indirectly from experimental data (as  $\rho_{min}^0$  and  $r$ ). Most of these measurements have not yet been performed; we hope that our work will motivate such experiments further examining the validity of our assumptions. In fact, one of the parameters,  $r^*/r_0$  was set to 1 during the fitting processes, as currently there is no available data to estimate its value. Our numerical results suggest that it is probably larger than 0.3, and it is unlikely to be larger than 2 (meaning an average lifetime less than 30 min). Within this range our qualitative conclusions are valid, while the numerical values of the parameter estimates can change up to a factor of 3.

The behavior of "precocious" swarming mutants reported in Ref. [9] deserves special attention. First we would like to comment on the huge difference found in the value of the transition rate  $r$  (see Table II). We emphasize that this is not an arbitrary output of a multiparameter fitting process.

First, we have reasons to believe that the motility thresholds of the two BB strains are rather similar. Knowing the growth rates and the cycle times, Eq. (12) shows us that the difference in the values of  $\rho_{min}$  cannot exceed one order of magnitude. Assuming then this maximal difference in  $\rho_{min}$ ,  $r$  remains the *only* free variable in Eqs. (13)–(15), and the fitting can be performed unambiguously. Thus, we are quite confident that such a large difference exists in  $r$  showing that the *rsbA* gene (in which these strains differ) influences not only the cell density threshold, but the rate of differentiation as well. It is also interesting to note that in Fig. 8(b) the behavior of the PRM2 and PRM1 strains reflect a relation very similar to that of the BB2000 and BB2235 strains. Finally, our calculations predicted a slightly longer cycle time for the precocious swarming mutant BB2235, which is also in accord with the actual experimental findings (see Fig 2 of Ref. [9]).

In our model the assumed functional form of the density dependence of the diffusion coefficient is somewhat different from the one most often considered [24,26], namely,

$$D(\rho) \sim \rho^k. \quad (17)$$

The advantage of Eq. (17) is that it allows analytic solutions for certain cases [21]; however, it describes an unlimited, arbitrarily fast diffusion inside the colony where the density is high. In contrast, in real colonies the diffusion of cells is certainly bounded, and the expansion of the boundary can be often limited by the supply of cells from behind [14]. Therefore we believe that our thresholded formulation [Eq. (7)] is a better approximation of what is taking place inside the real colonies.

Finally, we would like to comment on the role of nutrients in the swarming behavior of *P. mirabilis*. In our model there

is a phenomenological parameter ( $\tau$ ) determining how long the swarmer cells are produced at a given position in the colony. When investigating the dependence of the cycle time on this parameter, as Fig. 5 demonstrates, we found an extremely weak effect. Thus, at least within the framework of this model, there is no contradiction between the assumption that the swarmer cell *production* ceases due to nutrient (or accumulated waste) limitations, and the seemingly nutrient-independent cyclic behavior. In fact, this idea can be developed further. By increasing  $\tau$  (or decreasing the motility threshold  $\rho_{min}^*$ ) we arrive at a regime where the migration and consolidation phases are not clearly separable, as a motile swarmer cell population exists even when the expansion of the colony is slower. Experiments mapping the morphology diagram of *P. mirabilis* (Fig. 2 of Ref. [29]) showed that there are certain values of agar hardness and nutrient concentration, for which the expansion of the colony is still oscillating, but the periodic density changes are smeared out due to the presence of motile swarmer cells in the consolidation periods. If one associates the increasing agar hardness with increasing  $\rho_{min}^*$ , and the nutrient concentration with  $\tau$ , then one can qualitatively reproduce those (i.e., the  $P_r$  and  $P_h$ ) regions of the morphology diagram.

#### ACKNOWLEDGMENTS

One of the authors (M.M.) is grateful to T. Matsuyama and H. Itoh for many stimulating discussions on experimental results. This work was supported by funds OTKA T019299, F026645; FKFP 0203/197 and by Grant Nos. 09640471 and 11214205 from the Ministry of Education, Science and Culture of Japan.

- 
- [1] *Bacteria as Multicellular Organisms*, edited by J. A. Shapiro and M. Dworkin, (Oxford University Press, Oxford, 1997).
- [2] *Dynamics of Cell and Tissue Motion*, edited by W. Alt, A. Deutsch, and G. A. Dunn, (Birkhäuser, Basel, 1997).
- [3] G. Hauser, *Über Fäulnisbakterien und deren Beziehungen zur Septicämie* (Vogel, Leipzig, 1885).
- [4] F.D. Williams and R.H. Schwarzhoff, *Ann. Rev. Microbiol.* **32**, 101 (1978).
- [5] C. Allison and C. Hughes, *Sci. Prog.* **75**, 403 (1991).
- [6] G.M. Fraser and C. Hughes, *Curr. Opin. Microbiol.* **2**, 630 (1999).
- [7] C. Allison, H-C. Lai, D. Gygi, and C. Hughes, *Mol. Microbiol.* **8**, 53 (1993).
- [8] L. McCarter and M. Silvermann, *Mol. Microbiol.* **4**, 1057 (1990).
- [9] R. Belas, R. Schneider, and M. Melch, *J. Bacteriol.* **180**, 6126 (1998).
- [10] C. Fuqua, S.C. Winans, and E.P. Greenberg, *Annu. Rev. Microbiol.* **50**, 727 (1996).
- [11] J.A. Shapiro, *Annu. Rev. Microbiol.* **52**, 81 (1998).
- [12] F.D. Williams, D.M. Anderson, P.S. Hoffman, R.H. Schwarzhof, and S. Leonard, *J. Bacteriol.* **127**, 237 (1976).
- [13] T. Matsuyama, Y. Takagi, Y. Nakagawa, H. Itoh, J. Wakita, and M. Matsushita, *J. Bacteriol.* **182**, 385 (2000).
- [14] O. Rauprich, M. Matsushita, C.J. Weijer, F. Siegert, S.E. Esipov, and J.A. Shapiro, *J. Bacteriol.* **178**, 6525 (1996).
- [15] H. Itoh, J.-I. Wakita, T. Matsuyama, and M. Matsushita, *J. Phys. Soc. Jpn.* **68**, 1436 (1999).
- [16] A. Dufour, R.B. Furness, and C. Hughes, *Mol. Microbiol.* **29**, 741 (1998).
- [17] M. Matsushita (unpublished).
- [18] W.H. Press, S.A. Teukolsky, W.T. Vetterling, and B.P. Flannery, *Numerical Recipes*, 2nd ed. (Cambridge University Press, Cambridge, 1992).
- [19] M.C. Cross and P.C. Hohenberg, *Rev. Mod. Phys.* **65**, 2 (1993).
- [20] T. Antal, M. Droz, J. Magnin, Z. Rácz, and M. Zrinyi, *J. Chem. Phys.* **109**, 9479 (1998).
- [21] J.D. Murray *Mathematical Biology* (Springer-Verlag, Berlin, 1989).
- [22] L. Tsimring, H. Levine, I. Aranson, E. Ben-Jacob, I. Cohen, O. Shochet, and W.N. Reynolds, *Phys. Rev. Lett.* **75**, 1859 (1995).
- [23] D.E. Woodward, R. Tyson, M.R. Myerscough, J.D. Murray,

- E.O. Budrene, and H.C. Berg, *Biophys. J.* **68**, 2181 (1995).
- [24] I. Golding, Y. Kozlovsky, I. Cohen, and E. Ben-Jacob, *Physica A* **260**, 510 (1998).
- [25] M. Matsushita, J. Wakita, H. Itoh, K. Watanabe, T. Arai, T. Matsuyama, H. Sakaguchi, and M. Mimura, *Physica A* **274**, 190 (1999).
- [26] M. Mimura, H. Sakaguchi, and M. Matsushita, *Physica A* **282**, 283 (2000).
- [27] M.A. Bees, P. Andresen, E. Mosekilde, and M. Giskov, *J. Math. Biol.* **40**, 27 (2000).
- [28] S.E. Esipov and J.A. Shapiro, *J. Math. Biol.* **36**, 249 (1998).
- [29] A. Nakahara, Y. Shimada, J. Wakita, M. Matsushita, and T. Matsuyama, *J. Phys. Soc. Jpn.* **65**, 2700 (1996).